Article

MODIS Retrieval of Aerosol Optical Depth over Turbid Coastal Water

Yi Wang [1,2,3], Jun Wang [1,2,3,*], Robert C. Levy [4], Xiaoguang Xu [1,2], and Jeffrey S. Reid [5]

[1] Department of Chemical and Biochemical Engineering, The University of Iowa, Iowa City, IA 52242, USA; yi-wang-4@uiowa.edu (Y. W.); xiaoguang-xu@uiowa.edu (X. X.)
[2] Center of Global and Regional Environmental Research, The University of Iowa, Iowa City, IA 52242, USA
[3] Interdisciplinary Graduate Program in Informatics, The University of Iowa, Iowa City, IA 52242, USA
[4] NASA Goddard Space Flight Center, Greenbelt, MD 20771, USA; robert.c.levy@nasa.gov
[5] Marine Meteorology Division, Naval Research Laboratory, Monterey, CA 93943, USA; jeffrey.reid@nrlmry.navy.mil
* Correspondence: jun-wang-1@uiowa.edu; Tel.: +1-319-353-4483

Academic Editor: name
Received: date; Accepted: date; Published: date

Abstract: We present a new approach to retrieve Aerosol Optical Depth (AOD) from Moderate Resolution Imaging Spectroradiometer (MODIS) over the turbid coastal water. This approach supplements the operational Dark Target (DT) aerosol retrieval algorithm that currently don't conduct any AOD retrieval in the regions with large water-leaving radiances in the visible spectrum. Over the global coastal water regions in all cloud-free conditions, this unavailability of AOD retrievals due to the inherent limitation in existing DT algorithm is ~20%. Here, we refine the MODIS DT algorithm by considering that water-leaving radiance at 2.1 μm is negligible regardless of water turbidity. This refinement, with the assumption that the aerosol single scattering properties over coastal turbid water are similar to that over the adjacent open-ocean pixels, yields ~18% more of MODIS-AERONET collocated pairs for six AEROENT stations in the coastal water regions. Furthermore, comparison with these AERONET observations show that the new AOD retrievals are in either equivalent or better accuracy than those retrieved by the MODIS operational algorithm (over coastal land and non-turbid coastal water). Combining the new retrievals with the existing MODIS operational retrievals not only yield an overall improvement of AOD over those coastal water regions, but also successfully extend the spatial and temporal coverage of MODIS AOD retrievals over the coastal regions where 60% of human population resides, and thereby, aerosol impacts on regional air quality and climate are expected to be significant.

Keywords: AOD; coastal water; MODIS; retrieval

1. Introduction

Aerosols are a colloidal system of particles suspended in the atmosphere, and have significant impacts on weather, climate, and human health [1-3]. To quantify these impacts, satellite remote sensing has a critical observational role as it is the only approach to routinely retrieving aerosol properties such as the aerosol optical depth (AOD), with well-characterized uncertainty envelope, at high spatial resolution over the globe. Indeed, the near global coverage of Moderate Resolution Imaging Spectroradiometer (MODIS) AOD retrievals derived by Dark Target (DT) algorithm [4] or Deep Blue (DB) algorithm (land only) [5,6] have been used widely in the research community [7] since 2000 when MODIS aboard on Terra satellite started to collect the data.

One region of persistent challenge to aerosol remote sensing is the failure of algorithms to retrieve over coastal (or littoral) waters. Ocean color along coastlines has strong spectral and spatial variability leading poorly constrained lower boundary conditions. Yet, retrieving AOD in coastal

waters is an important and integral part toward better characterization of anthropogenic air pollution and aerosol radiative effects from space. Indeed, ~60% of human population lives in coastal areas [8], and the resultant emissions and effects of anthropogenic aerosols are difficult to observe. This study aims to address this observational gap by refining the MODIS DT-ocean algorithm to retrieve AOD over turbid coastal waters.

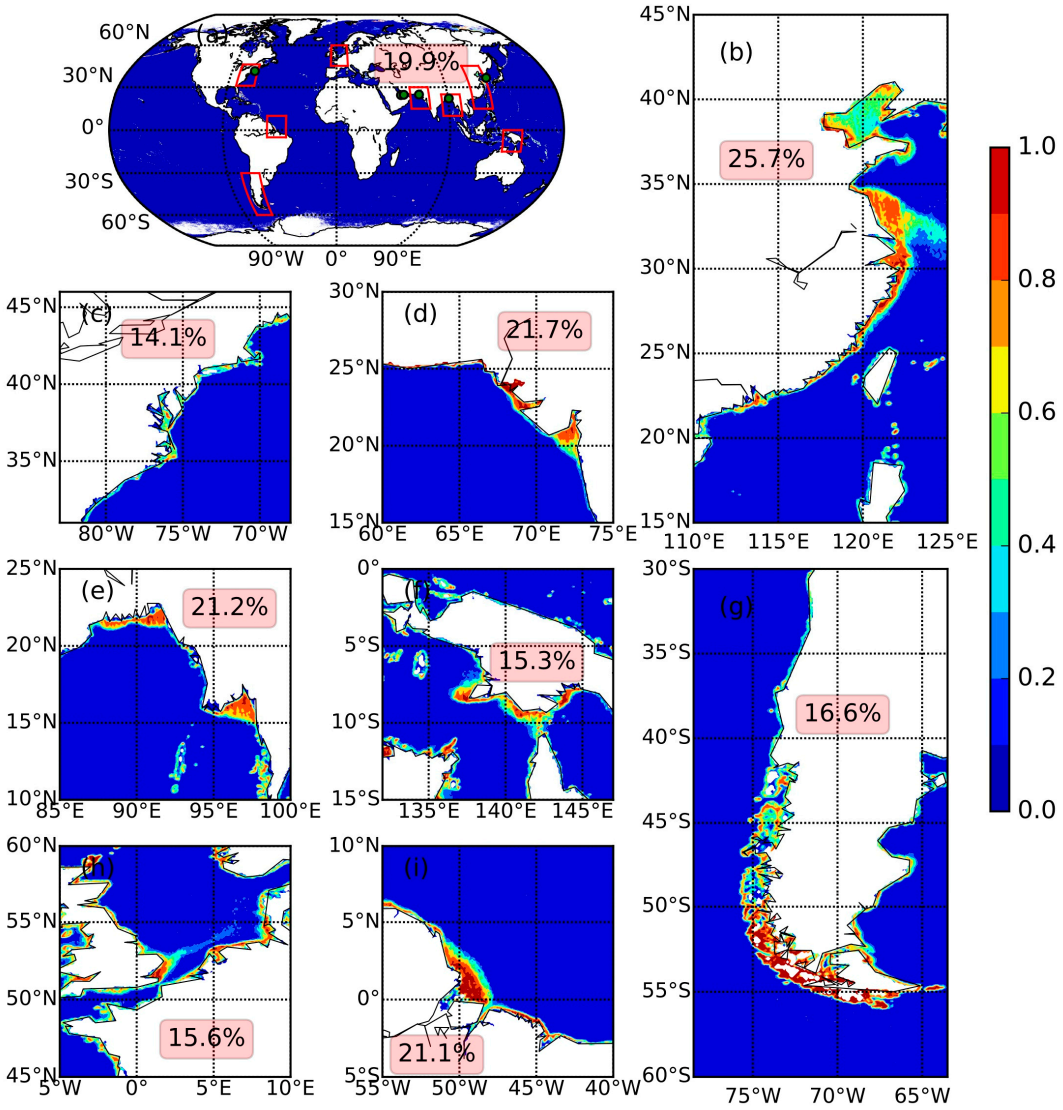

Figure 1. Global (**a**) and regional (**b-g**) distribution of AOD unavailable ratio which is defined as the ratio between number of non-retrieval pixels and all pixels in cloud-free condition. Zoom in on the red-box regions of (**a**) are shown in (**b-g**). Green points in (**a**) are AERONET sites used for validation and more information is in table 1. Numbers in the pink boxes are AOD unavailable ratio over coastal water in clear sky condition.

The MODIS DT-ocean algorithm uses top of atmosphere (TOA) reflectance at 6 bands ranging from 0.55 to 2.1 μm to simultaneously retrieve AOD and Fine Mode Fraction (FMF) based on a lookup table approach. The lookup table is constructed on 4 fine aerosol modes and 5 coarse aerosol modes with the assumptions of a rough ocean surface with zero water-leaving radiance at all bands except 0.55 μm (at which a fixed water-leaving reflectance of 0.005 is used) [4,9]. The retrieval process searches the lookup table to find the best combination of fine mode and coarse mode aerosol type (out of possibly 20 combinations) such that the AOD and FMF retrievals render the best match between observed and simulated (e.g., those from the lookup table) radiances. However, the assumption of nearly-zero water-leaving radiance is only suitable for open ocean but not applicable to turbid coastal water where the water-leaving radiances can be contributed by reflection of shallow-

water sea floor and either suspended or dissolved particulate matter in the water, especially at shorter wavelengths such as at 0.55, 0.66, and 0.86 μm [10]. Hence, as part of the DT-ocean algorithm, the turbid water pixels are masked and not considered for retrieval, even if these are cloud-free pixels. The method used for such masking compares the TOA reflectance at 0.55 μm with the expected counterpart from the power-law fitting using the TOA reflectance at 0.47, 1.2, 1.6, and 2.1 μm; if a significant difference (larger than 0.01) is found, the corresponding pixel is masked out for AOD retrieval [8].

Since the water turbidity changes slower in time than aerosol and cloud features, we analyze the MODIS AOD retrieval unavailability over the cloud-free conditions to reveal how often the AOD is not retrieved only because of water turbidity (not other factors such as cloud cover), at both global and regional scale. As shown in Figure 1, this data availability is near total over all open ocean and decreases dramatically (by 90-100%) toward coastlines. In a global average, the unavailability of AOD is ~20% over coastal water region which is labelled as shallow ocean (within 5 km of coastline or with water depth less than 50 m) in MODIS geolocation product [11]. In other words, in these 20% of cloud-free cases, the AOD should have been retrieved if there were not water turbidity problem.

Based on the principal that liquid water absorption increases in shortwave infrared (SWIR), we present a new approach that uses MODIS-measured radiance at 2.1μm to retrieve AOD over turbid coastal water no matter aerosol is fine or coarse mode dominated. In the spectral range of 0.55 to 2.1 μm, the transparency of pure water to sunlight decreases rapidly with the increase of wavelength; the penetration depth (at which light attenuation is 90%) is 41 m at 0.55 μm and reduces to 0.001 m at 2.1 μm [8]. Hence, the water-leaving radiance contributed from the sea floor, sediments, and other contaminants in the water at 2.1 μm is nearly negligible; this vastly simplifies the lower boundary condition of the retrieval. We present the data and the new approach in Section 2 and Section 3, respectively, followed by description of retrieval results and the validation against measurements from six Aerosol Robotic Network (AERONET) coastal sites in Section 4. Conclusions are in Section 5.

2. Data

MODIS is an earth-viewing sensor aboard on Terra and Aqua polar-orbiting satellites, launched in December 1999 and May 2002, respectively. It has 36 channels spanning the spectral range from 0.41 to 15 μm with spatial resolutions of 250 m (2 channels), 500 m (5 channels), and 1 km (29 channels). Its 2330-km swath width makes it able to provide near-global converge daily. Terra and Aqua cross the equator from north to south (descending node) at approximately 10:30 AM local time and from south to north (ascending node) at approximately 1:30 PM local time, respectively.

Here, all MODIS data products are labeled as MxDNN, where x is substituted by O for Terra and Y for Aqua, respectively, and NN is the serial number of a specific product. King et al. [12] presented a general description of MODIS atmosphere data processing architecture and products. In this study, MODIS calibrated TOA reflectance product (MxD02) (http://mcst.gsfc.nasa.gov/content/l1b-documents), atmospheric profile product (MxD07), geolocation product (MxD03), and aerosol product (MxD04) [4] are used for retrieving aerosol optical depth over turbid coastal water. 2.1 μm TOA reflectance with spatial resolution of 500 m from MxD02 is used to retrieve AOD through a lookup table (LUT) method. Gas absorption by water vapor and ozone column are corrected from the TOA reflectance with spatial resolution of 5 km from MxD07 product [4]. MxD03 product has a spatial resolution of 1 km and is used to distinguish between water and land pixels. All other ancillary information from MxD04 aerosol product for each valid AOD retrieval (at spatial resolution of 10 km at nadir) are also used as input to the retrieval algorithm in this study; the information includes aerosol mode index, reflectance weighting parameter, and National Centers for Environmental Prediction (NCEP) analysis of wind speed (2 m above the surface). In addition, cloud mask with spatial resolution of 500 m from MxD04 aerosol product is also used to ensure only AOD during cloud-free conditions over the turbid coastal region is retrieved by this study.

AOD measurements from the ground-based Aerosol Robotic Network (AERONET) are used for validating MODIS retrievals over coastal water in this study. All AERONET Sun Photometers (SP) measure direct solar radiation at 0.44 μm, 0.67 μm, 0.87 μm, 0.94 μm and 1.02 μm, and these measurements are used to infer AOD through Beer-Lambert-Bouguer law with quality at Level 1.0 (unscreened), Level 1.5 (cloud screened), and Level 2.0 (cloud-screened and quality-assured) [13,14]. We evaluate MODIS AOD (both MxD04 product and retrieval of this study) at 0.55 μm against AERONET counterpart that is derived through linear interpolating AERONET AOD at 0.44 and 0.67 μm in the logarithm domain.

Table 1. Information of AERONET sites used for validation

Site	Location*	Period	Data level	0.44-0.87 μm Ångström exponent
MVCO	41.3°N 70.6°W	August 2015	2.0	1.842
Bhola	22.2°N 90.8°E	December 2015	1.5	1.206
Anmyon	36.5°N 126.3°E	May 2016	1.5	1.076
Dalma	24.5°N 52.3°E	August 2004	2.0	0.711
Karachi	24.9°N 67.0°E	March 2014	2.0	0.701
MAARCO	24.7°N 54.7°E	September 2004	2.0	0.597

* All the locations are shown as green points in Figure 1a.

Information of 6 coastal AERONET sites used for evaluation is summarized in Table 1, and their locations are marked in global map in Figure 1a. Dalma and MVCO are two sites over the ocean with distance to coastline being 48 km and 29 km, respectively, while the rest sites are over land within 6 km from the coastline. According to our analysis, most AERONET sites are more than 10 km away from the coast lines, and lack dedicated long-term continuous measurements of AOD over the turbid coastal water. Here, we use the SP AOD data in August 2015, December 2015, May 2016, August 2004, March 2014, and September 2004 at MVCO Bhola, Anmyon, Dalma, Karachi, and MAARCO sites, respectively, because these time periods have most measurements available at their corresponding sites. AERONET Level 2.0 data are used for most sites except Bhola and Anmyon where only Level 1.5 data are available and utilized here. The monthly mean AERONET 0.44-0.87 μm Ångström exponent ranges from 0.597 to 1.842 over these seven sites. Hence, these sites represent a wide range of atmospheric conditions, ranging from coarse mode dominated to fine mode dominated cases [15].

3. Retrieval algorithm

3.1 Retrieval principal and sensitivity analysis

The new algorithm is based on lookup table (LUT) approach which is using observational TOA reflectance to fit the counterpart simulated hence finding the best-matching AOD. Thus, it is critical to determine the wavelength which has large sensor sensitivity with respect to AOD for retrieving. We compare the sensor sensitivity at 2.1 μm at which water-leaving radiance is negligible regardless of water turbidity with that at shorter wavelength which has large water-leaving radiance over turbid coastal water (taking 0.65 μm as an example). Figure 2 shows 2.1 μm TOA reflectance has larger sensor sensitivity than 0.65 μm in both fine and coarse mode aerosol situations when 0.65 μm surface reflectance is large (turbid coastal water). When aerosol optical depth is small (less than 0.15 at 0.55 μm, Figure 2b), we can use TOA reflectance (Figure 2c-d) to represents surface reflectance. Surface

Preprints (www.preprints.org) | NOT PEER-REVIEWED | Posted: 22 May 2017 doi:10.20944/preprints201705.0157.v1

Peer-reviewed version available at Remote Sens. 2017, 9, , 595; doi:10.3390/rs9060595

reflectance of turbid coastal water is up to 0.4 at 0.65 µm (Figure 2c) while it is very small (less than 0.0035) at 2.1 µm (Figure 2d). Figure 2e-h present simulation of TOA reflectance through UNL-VRTM model [16] with various surface reflectance in fine aerosol (average of the 4 fine aerosol modes defined in the DT-ocean LUT) and coarse aerosol (average of the 5 fine aerosol modes defined in the DT-ocean LUT) situations. In fine aerosol situation, 0.65 µm TOA reflectance is an increasing function of AOD when surface reflectance is small (0.03, clear water) (Figure 2e). However, it first decreases and then increases slowly when surface reflectance is large (0.3 or 0.4, turbid coastal water) (Figure 2f). The gradient of 2.1 µm MODIS digital signal (defined as change of MODIS digital count, $dn**$, with respect to 0.55 µm AOD, or $(\partial(dn**)_{2.1}/\partial\,(AOD)_{0.55})$ is ~25 no matter of AOD values (Figure 2j) while $\partial(dn**)_{0.65}/\partial\,(AOD)_{0.55}$ is smaller than 25 when AOD is less than 0.5 (1.2) and surface reflectance is 0.3 (0.4). This means it is better to use TOA reflectance at 2.1 µm rather than 0.65 µm to retrieve fine AOD in turbid coastal water situation. Further, even over surface water that is not turbid, while the sensitivity of 2.1 µm to the AOD change is a factor of 3-8 smaller than the counterpart at 0.65 µm (e.g., contrasts of blue lines between Fig. 2i and 2j), 2.1 µm still has significant sensitivity to the change of fine-mode AOD, and its detection limit for fine-mode AOD only is ~0.04 (e.g., the inverse of $\partial(dn**)_{2.1}/\partial\,(AOD)_{0.55}$). The reason that 2.1 µm still has reasonably good sensitivity for fine-mode aerosols is because the ocean surface is nearly black at 2.1 µm, albeit fine aerosol extinction decrease significantly.

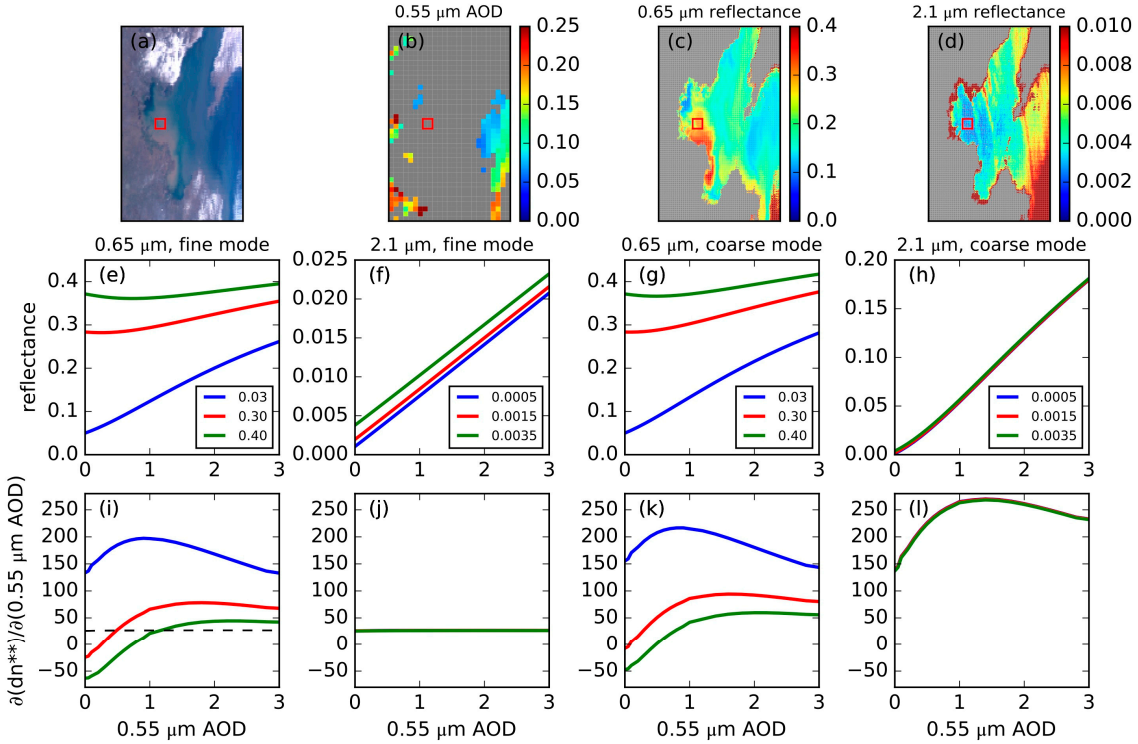

Figure 2. (**a**), (**b**), (**c**), and (**d**) are MODIS Aqua true color image, 0.55 µm AOD, 0.65 µm TOA reflectance, and 2.1 µm TOA reflectance at Bohai Sea, China on Feb. 23, 2017, respectively. Red box is the region where water is turbid and atmosphere is clean. (**e**) and (**f**) are simulation (solar zenith angle is 24°, view zenith angle 54°, and relative azimuth angle 60°) of 0.65 µm and 2.1 µm TOA reflectance with fine aerosol model, respectively. (**g**) and (**h**) are similar to (**e**) and (**f**) but coarse aerosol model. (**i**) and (**j**) are gradient of 0.65 µm and 2.1 µm MODIS digital signal (dn**) with respective to 0.55 µm AOD with fine aerosol model. (**k**) and (**l**) are similar to (**i**) and (**j**) but coarse aerosol model. Values in the legends are surface reflectance.

In coarse aerosol situation, $\partial(dn**)_{0.65}/\partial(AOD)_{0.55}$ is similar to that in fine aerosol situation and is a little smaller than $\partial(dn**)_{2.1}/\partial(AOD)_{0.55}$ when 0.65 μm surface reflectance is small (Figure 2k-l). However, $\partial(dn**)_{0.65}/\partial(AOD)_{0.55}$ is much a factor of 6-10 smaller than $\partial(dn**)_{2.1}/\partial(AOD)_{0.55}$ when water is turbid (e.g., contrast of red/green curves between Figure 2k and 2l). Overall, over turbid water, it is better to use TOA reflectance at 2.1 μm rather than 0.65 μm to retrieve AOD regardless if aerosol is dominated by fine or coarse mode, and it is apparent that 2.1 μm should be used to retrieve coarse-mode AOD regardless of water turbidity.

3.2 Algorithm implementation and steps

The retrieval algorithm is designed to supplement existing DT algorithm. Hence, the lookup table (LUT) from the MODIS DT-ocean AOD retrieval algorithm is used here [4,9]. The LUT is created by using the Ahmad and Fraser [17]'s radiative transfer code for various 0.55 μm AOD values in the range of 0 to 3 at different Sun-Earth-satellite geometries [4,9]. As water surface reflectance depends on surface wind speed, 4 wind speeds which includes 2 m s-1, 6 m s-1, 10 m s-1, and 14 m s-1 are assumed in the LUT construction. The LUT is computed for 4 fine aerosol modes (including 2 types of water insoluble and 2 types of water soluble) and 5 coarse aerosol modes (including 3 types of wet sea salt and 2 types of dusk-like aerosols (http://darktarget.gsfc.nasa.gov/algorithm/ocean/aerosol-models). Combination of a fine mode and a coarse mode is required in the DT algorithm for AOD retrieval and is also needed in the algorithm proposed here. In the retrieval procedure, MxD02 TOA reflectance at 2.1 μm is used to fit the corresponding LUT value $\rho_{2.1}^{\mathrm{LUK}}(\tau_{0.55}^{tot})$ which is a weighted sum of pure fine mode LUT value $\rho_{2.1}^{\mathrm{f}}(\tau_{0.55}^{tot})$ and pure coarse mode LUT $\rho_{2.1}^{\mathrm{c}}(\tau_{0.55}^{tot})$ at a given 0.55 μm AOD value $\tau_{0.55}^{tot}$.

$$\rho_{2.1}^{\mathrm{LUK}}(\tau_{0.55}^{tot}) = \eta\rho_{2.1}^{\mathrm{f}}(\tau_{0.55}^{tot}) + (1-\eta)\rho_{2.1}^{\mathrm{c}}(\tau_{0.55}^{tot}) \ , \qquad (1)$$

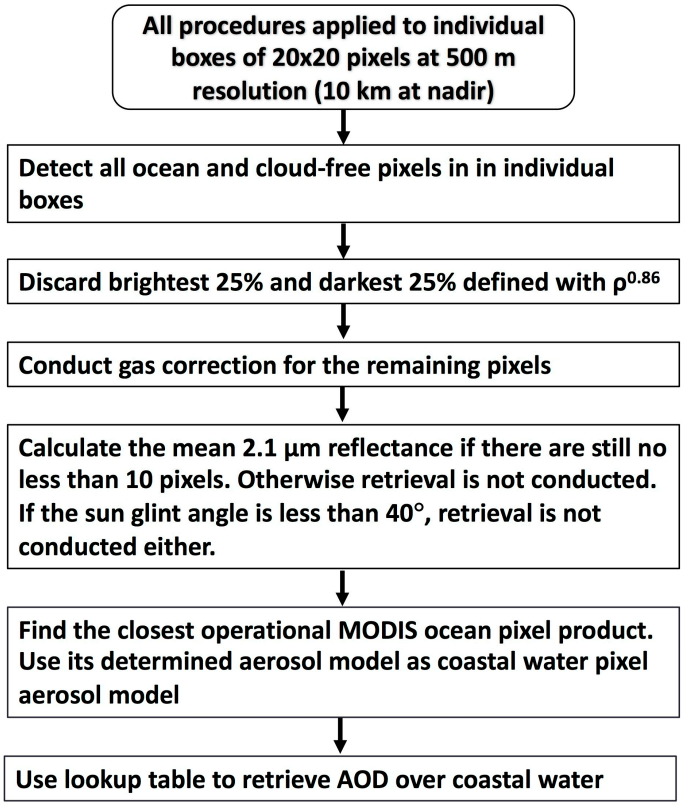

Figure 3. Flowchart of retrieving AOD over coastal water

The value of reflectance weighting parameter η equals the fraction of total AOD at 0.55 μm contributed by the fine mode [9]. In addition, the LUT is calculated under the assumption of "gas

free" (gas absorption is not included), thus correction [4] of MxD02 TOA reflectance is required to match the LUT before retrieving AOD.

Figure 3 shows the steps of our algorithm to retrieve AOD over coastal water, and hereafter, name this algorithm as Coastal Water (CW) algorithm. Each step of CW is described below with a note that these steps essentially follow DT-Ocean algorithm except CW uses the 2.1 um to retrieve AOD for those cloud-free turbid coastal water scenes as detected by the DT-Ocean algorithm. Hence, for each valid cloud-free turbid coastal water scene (e.g., a box of 20x20 pixels at 500 m resolution or at 10 km resolution at nadir, as available in the standard MODIS aerosol product), the following steps are implemented.

1. Discard the brightest 25% and darkest 25% pixels defined with 0.86 μm reflectance.
2. Conduct gas (H_2O, CO_2, and O_3) correction [4] for the remaining pixels.
3. Calculate the mean 2.1 μm TOA reflectance if there are still no less than 10 pixels. Otherwise retrieval is not conducted.
4. Calculate sun glint angle. If the sun glint angle is less than 40° retrieval is not conducted.
5. As we only use mean 2.1 μm reflectance to retrieve AOD, aerosol single scattering properties should be prescribed. Figure 4 shows that AOD can differ up to 0.2 in 100 km from the coast, but FMF differs only by 0.08 in 100 km from the coast. Thus, we assume the single scattering properties (including FMF) and surface wind speed for a turbid coastal water pixel is the same as those used for the AOD retrieval by the standard MODIS algorithm over its closest open-ocean pixel (within 100 km radius).
6. Use the mean 2.1 μm TOA reflectance and lookup table determined by equation (1) to retrieve AOD over the turbid coastal water where MxD04 product is unavailable. In application of equation (1), all ancillary information is obtained from step 5 except AOD.

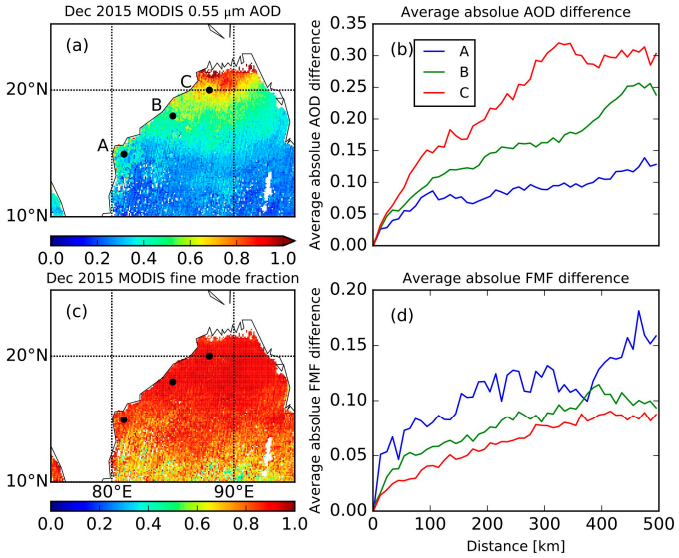

Figure 4. (**a**) and (**c**) are monthly mean 0.55 μm AOD and fine mode fraction (FMF) from MOD04 in December, 2015. (**b**) is average absolute AOD difference as a function a distance with respect to reference points (black solid circles in (**a**)). (**d**) is similar to (**b**), but for FMF.

4. Results

MxD04 [4] AOD and the AOD retrieval from CW algorithm are evaluated against AERONET measurements. The spatio-temporal matching approach by Ichoku, et al. [18] is applied to collocate AERONET AOD measurements and MODIS retrievals (MxD04 and/or CW) for comparison. AERONET measurements within ±30 minutes of the MODIS overpass time are averaged and compared against MODIS retrievals averaged within a 50-km diameter circular region centered over the AERONET sites. MxD04 products include DT, DB, and DT/DB merged retrievals, corresponding

Preprints (www.preprints.org) | NOT PEER-REVIEWED | Posted: 22 May 2017 doi:10.20944/preprints201705.0157.v1

Peer-reviewed version available at Remote Sens. 2017, 9, , 595; doi:10.3390/rs9060595

to 0.55 μm AOD from dark target algorithms (DT-land and DT-ocean algorithms), deep blue algorithm, and combination of the two retrievals, respectively [4]. DT retrievals cover both vegetated land and ocean while DB is limited to land. As DT-land algorithm is not designed to retrieve AOD over bright desert, there are significant amount of retrieval gaps over land. DB algorithm is originally designed to complement the gaps based on the principal that desert pixels are dark in deep-blue bands although they are bright in visible bands [5] and has been extended to vegetated land surface already. For this study, we use DB/DT merged product (Quality flag = 1, 2, 3 over ocean, and Quality flag = 3 over land) from MxD04. Thus, over the non-turbid ocean, essentially only AOD from DT is used.

An example of a granule over Bay of Bengal is shown in Figure 5. MxD04 AOD value is up to 1.6 in the center of the granule and decreases gradually southward, while retrievals are not available over coastal water of north part of the Bay of Bengal (Figure 5c). The non-retrieval region is in cloud-free condition (Figure 5a); AOD retrievals there should be available if it were not turbid water. Figure 5b shows that unavailability ratio over coastal water is 36.4% in cloud-free condition. The CW algorithm is applied to retrieve AOD over those turbid water condition. Figure 5d shows the combination of MxD04 and CW AOD, which means the CW AOD retrievals are used to fill where MxD04 are unavailable. Apparently, CW AOD retrievals enable a smooth and continuous distribution of AOD from MxD04 land AOD product to ocean AOD product. In addition, CW AOD retrievals are consistent with corresponding AERONET AOD value that is overlaid in Figure 5c and 5d.

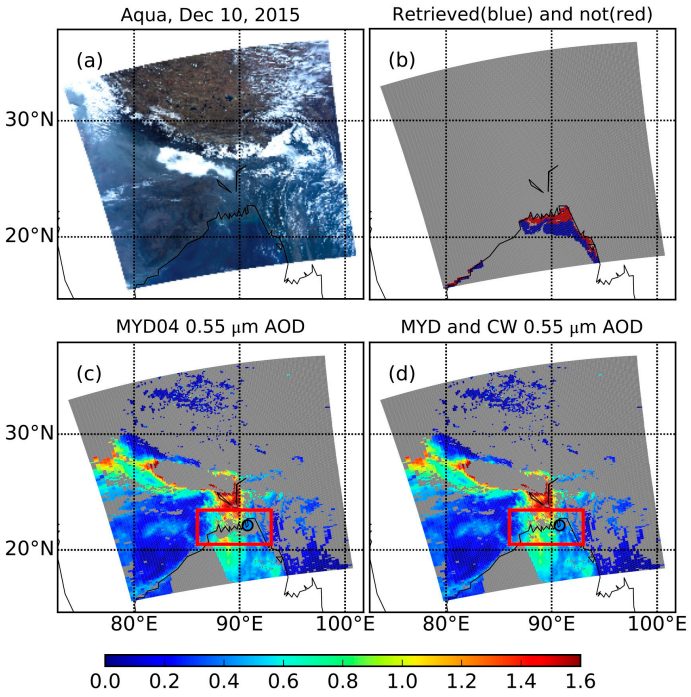

Figure 5. (**a**) Aqua MODIS true color image on December 10, 2015. (**b**) Blue and red represents coastal water where MYD AOD retrievals are available (blue) and unavailable (red), respectively in clear sky condition. (**c**) MYD04 0.55 μm DT/DB merged AOD retrievals. (**d**) is similar to (**c**), but the coastal water gaps where MYD04 AOD retrievals are not available in clear sky condition (red box) are filled by AOD retrievals from CW algorithm. AERONET AOD measurement overlaps on (**c**) and (**d**).

Both 0.55 μm AOD retrievals from MxD04 product and CW algorithm are evaluated against AERONET data (as shown in Figure 6). Figure 6a is a scatter plot of MxD04 retrievals versus AERONET measurements in the following two conditions: (a) all cloud-free pixels within 25 km radius proximity of AEROENT site are retrieved through MODIS operational algorithm or (b) only part of cloud-free pixels are retrieved through MODIS DT algorithm, but the AOD over the rest cloud-free pixels cannot be retrieved by CW algorithm because these pixels are over turbid water and no

Preprints (www.preprints.org) | NOT PEER-REVIEWED | Posted: 22 May 2017 doi:10.20944/preprints201705.0157.v1

Peer-reviewed version available at Remote Sens. 2017, 9, , 595; doi:10.3390/rs9060595

open-ocean pixel is close enough (e.g., within 100 km) to provide aerosol single scattering property for CW algorithm. Figure 6b is scatter plot of CW retrievals versus AERONET measurements in the scene that all cloud-free pixels within 25 km radius proximity of AEROENT site cannot be retrieved through MODIS DT-Ocean algorithm but some or all of them can be retrieved through CW algorithm. Comparison of Figure 6a and 6b shows that normalized mean bias (NMB) and root mean square error (RMSE) of CW algorithm (12.0% and 0.141) are smaller than that of MxD04 (15.9% and 0.213). The percentage of collocated pairs within expected error envelope and correlation coefficient increase from 35.5% and 0.72 in MxD04 only scene (Figure 6a) to 39.3% and 0.94 in CW only scene (Figure 6b), respectively.

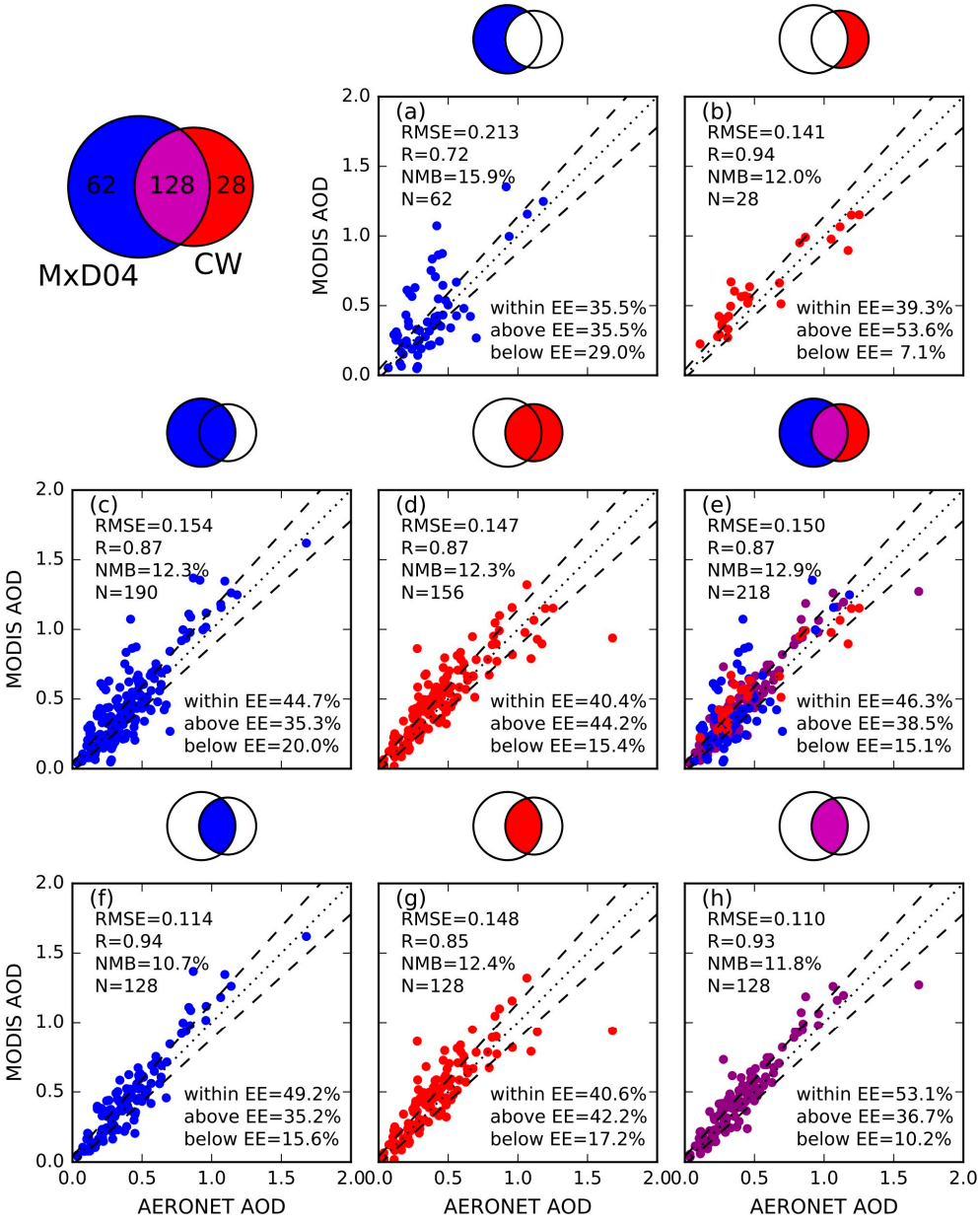

Figure 6. Scatter plots of 0.55 μm AOD retrievals from MODIS (MxD04 and/or CW) versus AERONET observations for the 12 monthly cases. Venn diagram on the upper left represents number of collocated data sets for MxD04-AEROENT (blue), CW-AERONET (red), (MxD04+CW)-AERONET (purple). Color part of Venn diagram on the top of each scatter plot represents which collocated data sets are plotted. 1:1 lines and expected error (EE) envelopes (+(0.04+10%), -(0.02+10%), asymmetric) are plotted as dot and dashed lines. The number of collocated pairs (N), root mean square error (RMSE), normalized mean bias (NMB), and linear correlation coefficient (R) are also shown.

Preprints (www.preprints.org) | NOT PEER-REVIEWED | Posted: 22 May 2017 doi:10.20944/preprints201705.0157.v1

Peer-reviewed version available at Remote Sens. 2017, 9, , 595; doi:10.3390/rs9060595

In addition to MxD04 only and CW only scene, there is a third situation that some of the cloud-free pixels are retrieved through operational MODIS algorithm while the CW algorithm is applied to the rest. Figure 6c and 6d are similar to 6a and 6b, respectively, but both include the AOD retrievals from their respective counterparts of the third situation. Overall, for all possible retrievals by each algorithm, CW retrievals are comparable to MxD04 in quality, although the MODIS operational algorithm have slight more samples.

The basis of MODIS-AERONET collocation is that air mass is always in motion and the average of MODIS AOD retrievals in a certain area which encompass a AERONRT site should be comparable to the temporal statistics of the AERONET measurements [18]. Therefore, we further show the inter-comparison between either MxD04 or CW AOD with AERONET AOD for cases where both MxD04 and CW are available (Figure 6h). The percentage of collocated pairs in the EE for (MxD04+CW) combined vs. AERONET (53.1%) is larger than that of MxD04-AERONET (49.2%, Figure 6f) and CW-AERONET (40.6%, Figure 6g). The RMSE of (MxD04+CW)-AERONET (0.110) is smaller than that of MxD04-AERONET (0.114) and CW-AERONET (0.148).

Inter-comparison of MxD04 and CW merged AOD with AERONET AOD is shown in the Figure 6e; such merged AOD include all data points in Figure 6a, 6b, and 6h. The number of collocated pairs increases from 190 (62 in MxD04 only scene plus 128 in combination scene) to 218 (total scene). In addition, the inter-comparison statistics (Figure 6e) is still comparable to or better than those retrieved from MxD04 only (Figures 6a and 6c) in quality. Overall, CW retrievals supplement MODIS DT, and improve the AOD retrievals both spatially and temporally without degrading (and sometimes increasing) the DT-Ocean AOD retrieval quality.

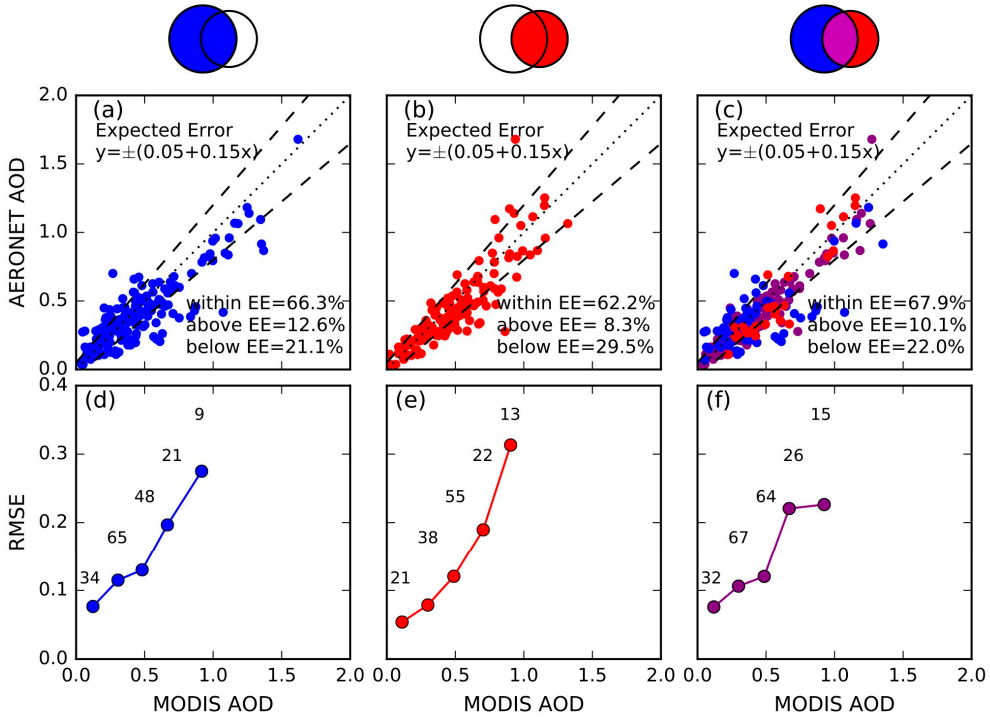

Figure 7. (**a**), (**b**), and (**c**) are scatter plots of AERONET 0.55 μm AOD observations versus retrievals from MODIS (MxD04 and/or CW) for the 12 monthly cases. Sampling method is same as in Figure 6. 1:1 lines and expected error (EE) envelopes (+(0.05+15%), -(0.05+15%), symmetric) are plotted as dot and dashed lines. (**d**), (**e**), and (**f**) are root mean square error (RMSE) as a function of MODIS AOD in the 0.2 interval. Numbers above averaged dot show how many AERONET-MODIS collocations are available to calculate RMSE.

In addition to evaluation of MODIS AOD diagnostic error in Figure 6, prognostic error is presented in Figure 7. Two thirds of AERONET-MODIS collocations are within the expected error envelope (y=±(0.05+0.15x)) (Figure 7c), thus 0.05+0.15(MODIS AOD) can be considered as its

prognostic error. Figure 7d-f show RMSE as a function of MODIS; RMSE goes up as MODIS AOD increases and combined retrievals (Figure 7f) are comparable to MxD04 (Figure 7d).

5. Conclusions

DT algorithm has been applied to retrieve AOD over land and ocean for MODIS sensors since early 2000. Although there are significant improvements on the algorithm in the past more than one decade, it does not retrieve AOD over turbid coastal water due to high water-leaving radiance in turbid water at visible bands. We designed Coastal Water AOD retrieval algorithm (CW algorithm) for these regions to supplement current DT algorithm. The AOD retrieval algorithm for turbid coastal water takes advantage of the fact that water-leaving radiance is negligible at 2.1 μm, hence only using this band to retrieve while other auxiliary information such as aerosol single scattering properties are obtained from DT retrievals over the nearby non-turbid water surfaces. In other words, the aerosol modes and reflectance weighting parameter of pixel to be retrieved is substituted by the closest counterpart from MxD04 ocean AOD product.

CW algorithm not only fills the gaps of MxD04 AOD retrievals over turbid coastal water but also improve their comparison with AERONET measurements. CW AOD retrievals are validated against measurements of six AERONET sites that are located at coastal regions. The new algorithm yields ~18% more of MODIS-AERONET collocated pairs, and CW AOD retrievals are better than or comparable to MxD04 in quality. In the case that both AOD retrievals from MxD04 and CW are available within 50 km diameter circular regions centered at AERONET sites, the merged AOD retrievals show better agreement with AERONET AOD either of them alone, in terms of the percentage of collocated pairs in the EE and RMSE.

While a new method is developed, and shows its complementary with existing DT-Ocean algorithm, it can be further evaluated with more AERONET sites (possibly through field campaigns). Further evaluation can also be targeted at the assumptions regarding the use of aerosol single scattering properties from adjacent non-turbid water pixels within certain threshold distance. Nevertheless, retrieval algorithm has to make assumptions, albeit sometimes such assumptions are empirically based. As MODIS sensors aboard on Terra and Aqua have been providing data for more than one decade and will be decommissioned by the early 2020s, its aerosol record is expected to be continued by the Visible Infrared Imaging Radiometer Suite (VIIRS) on board Suomi-NPP (S-NPP) which was launched late 2011. Thus, future investigate will also include the application of the approach in this study to VIIRS. VIIRS has 2.26μm band at which water leaving radiance is also negligible like 2.1μm band on MODIS.

Acknowledgments: Funding for this study was provided by the NASA Earth Science Division as part of NASA's Terr/Aqua and VIIRS science team program (grant numbers: NNX16AT63G and NNX17AC94A) as well as was supported by Office of Naval Research (ONR's) Multidisciplinary University Research Initiatives (MURI) Program under the award N00014-16-1-2040.

Author Contributions: Yi Wang, Jun Wang and Robert C. Levy conceived and designed the experiments; Yi Wang and Xiaoguang Xu performed the experiments and analyzed the data; Yi Wang and Jun Wang wrote the paper; Jeffrey S. Reid provided guidance to the project, reviewed and edited the paper.

Conflicts of Interest: The authors declare no conflict of interest.

References

1. Haywood, J.; Boucher, O. Estimates of the direct and indirect radiative forcing due to tropospheric aerosols: A review. *Rev. Geophys.* **2000**, *38*, 513-543.
2. Rosenfeld, D.; Lohmann, U.; Raga, G.B.; Dowd, C.D.; Kulmala, M.; Fuzzi, S.; Reissell, A.; Andreae, M.O. Flood or drought: How do aerosols affect precipitation? *Science* **2008**, *321*, 1309.
3. Lim, S.S.; Vos, T.; Flaxman, A.D.; Danaei, G.; Shibuya, K.; Adair-Rohani, H.; AlMazroa, M.A.; Amann, M.; Anderson, H.R.; Andrews, K.G., *et al.* A comparative risk assessment of burden of disease and injury

attributable to 67 risk factors and risk factor clusters in 21 regions, 1990–2010: A systematic analysis for the global burden of disease study 2010. *The Lancet* **2012**, *380*, 2224-2260.

4. Levy, R.C.; Mattoo, S.; Munchak, L.A.; Remer, L.A.; Sayer, A.M.; Patadia, F.; Hsu, N.C. The collection 6 modis aerosol products over land and ocean. *Atmos. Meas. Tech.* **2013**, *6*, 2989-3034.
5. Hsu, N.C.; Jeong, M.J.; Bettenhausen, C.; Sayer, A.M.; Hansell, R.; Seftor, C.S.; Huang, J.; Tsay, S.C. Enhanced deep blue aerosol retrieval algorithm: The second generation. *J. Geophys. Res.* **2013**, *118*, 9296-9315.
6. Sayer, A.M.; Hsu, N.C.; Bettenhausen, C.; Jeong, M.J. Validation and uncertainty estimates for modis collection 6 "deep blue" aerosol data. *J. Geophys. Res.* **2013**, *118*, 7864-7872.
7. IPCC. *Climate change 2013: The physical science basis. Contribution of working group i to the fifth assessment report of the intergovernmental panel on climate change*. Cambridge University Press: Cambridge, United Kingdom and New York, NY, USA, 2013; p 1535.
8. Li, R.-R.; Kaufman, Y.J.; Gao, B.-C.; Davis, C.O. Remote sensing of suspended sediments and shallow coastal waters. *IEEE Trans. Geosci. Remote Sens.* **2003**, *41*, 559-566.
9. Remer, L.A.; Kaufman, Y.J.; Tanré, D.; Mattoo, S.; Chu, D.A.; Martins, J.V.; Li, R.R.; Ichoku, C.; Levy, R.C.; Kleidman, R.G., *et al.* The modis aerosol algorithm, products, and validation. *J. Atmos. Sci.* **2005**, *62*, 947-973.
10. Anderson, J.C.; Wang, J.; Zeng, J.; Leptoukh, G.; Petrenko, M.; Ichoku, C.; Hu, C. Long-term statistical assessment of aqua-modis aerosol optical depth over coastal regions: Bias characteristics and uncertainty sources. *Tellus B; Vol 65 (2013)* **2013**.
11. Wolfe, R.E.; Nishihama, M.; Fleig, A.J.; Kuyper, J.A.; Roy, D.P.; Storey, J.C.; Patt, F.S. Achieving sub-pixel geolocation accuracy in support of modis land science. *Remote Sens. Environ.* **2002**, *83*, 31-49.
12. King, M.D.; Kaufman, Y.J.; Tanré, D.; Nakajima, T. Remote sensing of tropospheric aerosols from space: Past, present, and future. *Bull. Am. Meteorol. Soc.* **1999**, *80*, 2229-2259.
13. Smirnov, A.; Holben, B.N.; Eck, T.F.; Dubovik, O.; Slutsker, I. Cloud-screening and quality control algorithms for the aeronet database. *Remote Sens. Environ.* **2000**, *73*, 337-349.
14. Holben, B.N.; Eck, T.F.; Slutsker, I.; Tanré, D.; Buis, J.P.; Setzer, A.; Vermote, E.; Reagan, J.A.; Kaufman, Y.J.; Nakajima, T., *et al.* Aeronet—a federated instrument network and data archive for aerosol characterization. *Remote Sens. Environ.* **1998**, *66*, 1-16.
15. O'Neill, N.T.; Eck, T.F.; Smirnov, A.; Holben, B.N.; Thulasiraman, S. Spectral discrimination of coarse and fine mode optical depth. *J. Geophys. Res.* **2003**, *108*, 4559.
16. Wang, J.; Xu, X.; Ding, S.; Zeng, J.; Spurr, R.; Liu, X.; Chance, K.; Mishchenko, M. A numerical testbed for remote sensing of aerosols, and its demonstration for evaluating retrieval synergy from a geostationary satellite constellation of geo-cape and goes-r. *J. Quant. Spectrosc. Radiat. Transf.* **2014**, *146*, 510-528.
17. Ahmad, Z.; Fraser, R.S. An iterative radiative transfer code for ocean-atmosphere systems. *J. Atmos. Sci.* **1982**, *39*, 656-665.
18. Ichoku, C.; Chu, D.A.; Mattoo, S.; Kaufman, Y.J.; Remer, L.A.; Tanré, D.; Slutsker, I.; Holben, B.N. A spatio-temporal approach for global validation and analysis of modis aerosol products. *Geophys. Res. Lett.* **2002**, *29*, MOD1-1-MOD1-4.